ELSEVIER

Earth and Planetary Science Letters 205 (2003) 211–224

EPSL

www.elsevier.com/locate/epsl

Spatial variations of flexure parameters over the Tibet–Quinghai plateau

C. Braitenberg [a,*], Y. Wang [b], J. Fang [b], H.T. Hsu [b]

[a] *Department of Earth Sciences, University of Trieste, Via Weiss 1, 34100 Trieste, Italy*
[b] *Institute of Geodesy and Geophysics, Chinese Academy of Sciences, Xu Dong Road 54, 430077 Wuhan, PR China*

Received 29 July 2002; received in revised form 21 October 2002; accepted 22 October 2002

Abstract

We investigate the Tibet–Quinghai plateau and the Tarim basin in terms of spatial variations of the elastic thickness (T_e) in the frame of the thin plate flexure model. The method of investigation makes use of a convolutive method, which allows high spatial resolution of the flexure properties and overcomes some of the problems tied to the spectral admittance/coherence methodologies. We study the relation between the topographic and subsurface loads and the observed crust–mantle interface (CMI) undulations, the latter having been obtained from gravity inversion. The gravity data used for the inversion are a unique set of high quality data available over the Chinese part of the plateau, and constitute the highest resolution grid today available in this impervious area. The gravity inversion is constrained by results from the study of the propagation of seismic waves. The two extensive sedimentary basins, the Tarim and the Qaidam basins, are modeled by forward gravity modeling. The oscillations of the CMI obtained from the gravity inversion agree well with those expected by loading the thin plate model of spatially variably elastic thickness with the surface and subsurface loads. It is found that the modeling of the sedimentary basins is essential in the flexure analysis. The spatial variations of elastic thickness correlate with the extensions of the different terrains that constitute the plateau. Most of the Tibet plateau has low T_e, varying in the bounds 10–30 km, with lower values in the Qiangtang terrain, where the T_e reaches 8 km. The Tarim and the Qaidam basins, Precambrian platforms overlain by sediments, are rigid and have a T_e of up to 110 km and 70 km, respectively. The flexural analysis distinctly discerns the Tibet plateau, with thick crust, part of which is molten, from the cratonic areas, the Tarim and Qaidam basins, which though of thinner crust, act as undeformable rigid blocks.

Keywords: Quinghai–Tibet plateau; Tarim plate; gravity inversion; flexural isostasy; elastic thickness; crust–mantle interface

1. Introduction

The investigated area regards the plateau of Tibet and Quinghai, whose 5000 m average height makes it an interesting topic for isostasy studies. Fig. 1 shows the topographic map of the area, and the main features are recognized: the massive plateau, which along its southern and western edge is delimited by the Himalayas, to the North by the Kun Lun Range and the extensive Tarim basin, the latter being delimited by the Tien Shan

* Corresponding author. Tel.: +39-40-558-2258; Fax: +39-40-575-519.
E-mail address: berg@units.it (C. Braitenberg).

0012-821X/02/$ – see front matter
PII: S0012-821X(02)01042-7

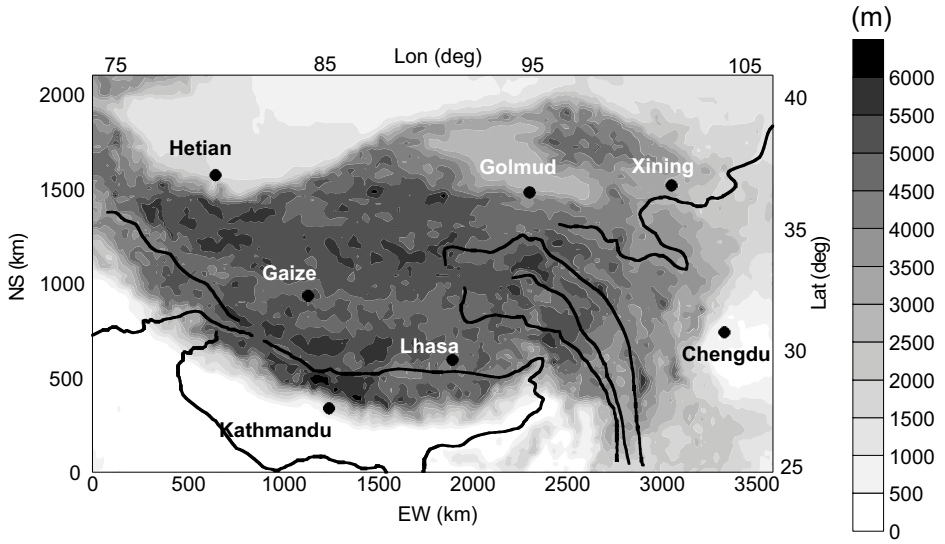

Fig. 1. Topography of Tibet–Quinghai plateau. Main towns and rivers are shown.

range towards the North. The further important depression is the Qaidam basin to the northeast of the plateau. In Fig. 2 the main structural lines are reported, which are the Main Boundary thrust, the Jarlung Zangbo suture, the Bang Gong Nujiang suture, the Jin Sha Suture, the Kunlun suture, and the Altyn Tagh fault.

Starting from the 1980s the crustal structure of Tibet has been investigated by geophysical studies in the frame of the GGT, PASSCAL and INDEPTH/GEDEPTH projects. The best studied area refers to the SW–NE trending profile AA′ (Fig. 2) connecting Lhasa and Golmud. The Tibet crust was found to be about 70–80 km

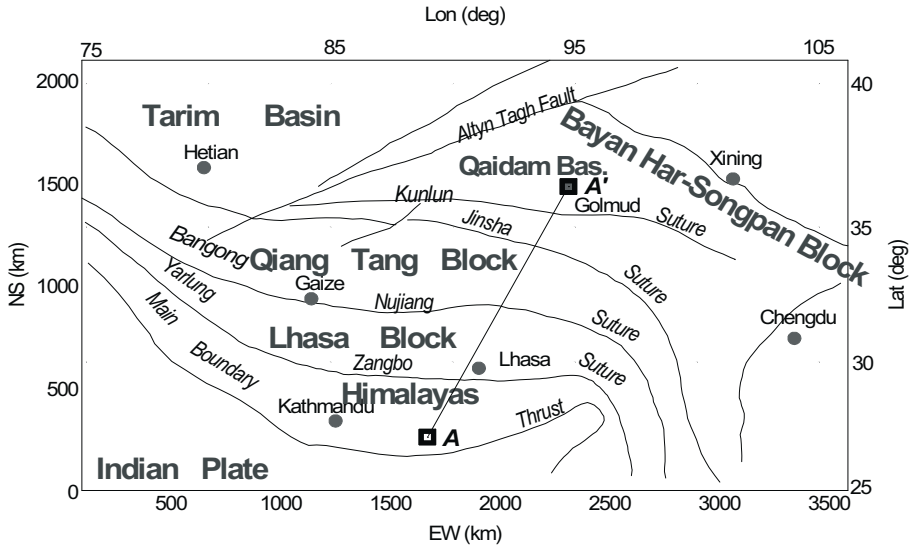

Fig. 2. Main structural elements and main tectonic lines in the Tibet–Quinghai plateau. The profile AA′ is discussed in the text.

thick with a probably partially molten crust beneath the depth of 20–30 km, characterized by high conductivity and a seismic low-velocity zone [1–6].

Our investigation of the Tibet–Quingahi plateau is made in the frame of an Italian–Chinese cooperation project started in 1997, that in its first stage achieved the inversion of the observed Bouguer gravity data in terms of crustal thickness variations over the entire Tibet plateau [7,8]. The present paper reports on the results from the second stage of the cooperation that includes a refinement of the crustal thickness model, by taking into account the gravitational effect of extensive superficial structures (e.g. basins). Furthermore, the observations are used to formulate an isostatic thin plate flexure model (e.g. [9]).

Regarding the model of thin plate isostatic compensation, the Tibet–Quinghai plateau and neighboring areas have been studied in the past by several authors. The Western Himalayas and the Karakoram Range, including parts of the Tarim basin, have been investigated by Lyon-Caen and Molnar [10], and Caporali [11–13]. Lyon-Caen and Molnar [10] model the observed gravity values along a profile across the Tarim basin and reaching the Kun Lun range by a flexing plate of constant $T_e = 40$ km (flexural rigidity 5×10^{23} Nm), and local type compensation ($T_e = 0$ km) starting from about 100 km SE of the Tarim basin. Caporali [11–13] studies the Bouguer and topography along profiles crossing the Karakoram and Western Himalaya and reaching into the Tarim plate. The Tarim plate is found to be considerably more rigid than the Karakoram Range. From spectral analysis it is inferred that in the Western Himalaya and Karakoram the lithosphere is rheologically layered, with a strong upper crust and upper mantle separated by a weak lower crust.

The Himalayan range was studied by Lyon-Caen and Molnar [14], Karner and Watts [15] and Royden [16] along profiles extending from the Ganga basin across the Himalayas into the southern portion of the Tibetan plateau. The studies agree essentially in modeling the observed Bouguer values with the flexure of the underthrusting Indian plate by the load of the sediments of the foreland basin and the weight of the mountain range. The Indian plate is estimated to have a T_e of 80–100 km. Lyon-Caen and Molnar [14] find a decrease of T_e beneath the Greater Himalaya to values of 10–20 km. The Tibet plateau was investigated with the pioneering works of Jin et al. [17,18]. The average admittance and coherence curves between the topography and Bouguer fields were estimated over a rectangular area covering the central part of the plateau and were modeled by a constant T_e lying between 40 and 50 km. Correlation studies of the topography and the Bouguer gravity fields suggested the presence of a weak decoupling zone between the Tibetan crust and upper mantle [17]. The forward modeling of the Bouguer gravity field along six profiles crossing Tibet was made with a 2D flexural model, where the elastic plate was allowed to have variable T_e. The plate was modeled as being composed of the Eurasian and the Indian plates, separated by a suture fault. The Indian plate has higher values of T_e to the south (90 km), below the Ganga plain, decreasing to a value of 30 km below the plateau. The value of the Eurasian plate is 45 km in Tarim, decreasing to 35 km below the plateau [18]. Burov and Diament [19] investigate the flexure over the Tarim basin by 2D analysis using the model of a multilayered crust and lithosphere and non-linear mechanical parameters. The crust and mantle are divided each into a brittle, elastic and ductile layer. They show that the non-linear and linear elastic modeling lead to essentially the same results, as long as the second derivative of flexure is less than about 10^{-7} 1/m. The 2D linear modeling predicts an elastic thickness of near to 60 km, which produces essentially the same results as the non-linear modeling, where the CMI is set at 50 km depth, the crustal part of the lithosphere has zero strength below 20 km, and the lithosphere has zero strength below 120 km depth.

Although the Tibet plateau and surrounding areas have been studied before by flexure analysis, these studies were limited to profiles. In the present work the 2D spatial variations of T_e in the entire Tibet and surrounding areas are modeled, which overcomes the problems that arouse in comparing T_e values obtained with different

methodologies and model parameters. The model we use in the flexure analysis is as follows. The lithosphere is assumed to deform elastically in response to sufficiently old loads ($>10^6$ yr) according to the thin plate model. The flexural rigidity of the lithosphere is allowed to vary spatially. The lithosphere is allowed to have density variations that are considered as internal loads and added to the external topographic load. The usefulness of the investigations of T_e has been illustrated by Burov and Diament [20], who developed an analytical and numerical approach to explain T_e in terms of the lithospheric rheology, thermal structure, and strain/stress distribution, allowing a means to constrain the lithospheric structure from estimates of T_e.

The flexure modeling is accomplished in the spatial domain in a manner similar to the one proposed in Watts et al. [21], pursued later by Cazenave et al. [22], and the T_e is modeled in 2D. The methodology involves the convolution of the load with the point load response function of the elastic plate model, obtaining the model flexure. The model flexure is compared to the observed flexure of the lithosphere. The observed flexure of the lithosphere is assumed to be equal to the CMI undulations, which are obtained by gravity inversion. All geophysical constraints regarding structure or geological models, from which density variations can be desumed, are taken into account in order to obtain a model of the CMI undulations by inversion of the observed gravity data.

We adopt a modified version of the CMI depth model reported in Braitenberg et al. [7] that is the result of a gravity inversion with the constraint of active and passive seismic investigations. In the improved version, the gravity effects of the two great sedimentary basins, the Tarim and Qaidam basins, are computed by 3D forward modeling, relying on existing models of the densities and depths of the basins.

2. Inverse modeling of the spatial variations of flexural properties

The thin plate flexure model predicts that the outermost layers of the earth respond to long term loads (>1 Myr) analogous to a thin elastic plate overlying an inviscid fluid. The loads are made up of the sum of the topographic and subsurface loads. The flexure $w(\vec{r})$, with $\vec{r}=(x,y)$, of the plate loaded by a load $h(\vec{r})$, in frequency–space is defined by (e.g. [9,23]):

$$W(\vec{k}) = \frac{\rho_c}{\rho_m - \rho_c + \frac{D}{g}|\vec{k}|^4} H(\vec{k}) \quad (1)$$

Where $W(\vec{k})$ is the Fourier transform (FT) of the flexure $w(\vec{r})$ of the median line of the plate, $H(\vec{k})$ is the FT of topography, ρ_m, ρ_c are respectively the crust and mantle densities, g is the normal gravity, $\vec{k}=(k_x, k_y)=2\pi(\nu_x, \nu_y)$ is the two-dimensional wave number, ν_x and ν_y are the spatial frequencies along the x- and y-axis, respectively, and D is the flexural rigidity of the plate, which is a function of Young's modulus E, the Poisson ratio σ, and the equivalent elastic thickness T_e as:

$$D = \frac{ET_e^3}{12(1-\sigma^2)} \quad (2)$$

In our paper we refer to the elastic thickness instead of to the flexural rigidity, which implies a choice of a rheological model. We refer to standard values with $E=10^{11}$ Pa and $\sigma=0.25$. The elastic thickness must be scaled accordingly for a different choice of the rheological model.

By taking the Fourier inverse transform of Eq. 1, the relation between the two quantities is given in space by the relation:

$$w(\vec{r}) = s(\vec{r}) * h(\vec{r}) \quad (3)$$

which is the convolution product of the load $h(\vec{r})$ with the point load flexure response function $s(\vec{r})$.

In the thin plate flexure model, it is generally assumed that the flexure $w(\vec{r})$ approximately equals the deviations from the flatness of the CMI. By using a series of flexure response functions in the convolution, each corresponding to a value of T_e between 0 km and 110 km, with a step of 0.5–10 km, we obtain the corresponding undulation of the flexure CMI. In order to compute the spatial variations of T_e, the root mean square

(rms) difference between the observed CMI and the flexure CMI undulations can be determined on square windows of side lengths L. The inverted T_e for the specific window is the one that minimizes the rms error, and thus achieves the best-fit approximation of the observed CMI. A detailed description of the flexural modeling by the convolution method is made in Braitenberg et al. [24], where the methodology was tested on a synthetic model and applied to the Eastern Alps.

3. The model of the depth to the CMI

As shown above, the modeling of the T_e is made by a best fit of the flexure CMI with an independent CMI model. Over Tibet observed terrestrial gravity data and seismological constraints on the crustal structure were combined to formulate a solution of the undulations of the CMI [7,8]. We refer to these two papers for details on the gravity database and the modeling. The CMI was obtained by application of an iterative hybrid spectral–classical inversion approach which has already been extensively tested on synthetic models [25] and in various geographical areas as the Alps [26–28] and Karakorum [29]. The method is an alternative to the approaches of Oldenburg [30] and Granser [31].

3.1. The basins

An improvement with respect to the CMI model of Braitenberg et al. [7,8] was achieved by taking advantage of the fact that now a model of the two great sedimentary basins, the Tarim and Qaidam basins, is available. The Tarim and Qaidam basins, having great horizontal extensions and considerable thickness, affect the gravity field considerably. Although in gravity inversion studies the fields due to superficial and deep masses can be separated respectively by frequency filtering to a certain extent (e.g. [32]), the separation fails with very extensive structures. It was shown by Jin et al. [17] that gravity variations in the Tibet area longer than 150–200 km are likely due to masses seated at depths of 50–100 km, that is at CMI level. In Braitenberg et al. [7,8] the gravity effect of the sediments was reduced by frequency filtering the observed gravity field, according to the results of Jin et al. [17], at a wavelength of 200 km. The two basins being of such large extent (2000 km and 700 km length for the Tarim and Qaidam basin, respectively), the frequency filtered gravity data were still affected by the influence of the basins. Models of the basin thickness are now available to us on a 0.5 by 0.5 degree grid that was obtained by integrating a large number of seismic exploration lines [33]. In Fig. 3 the basin

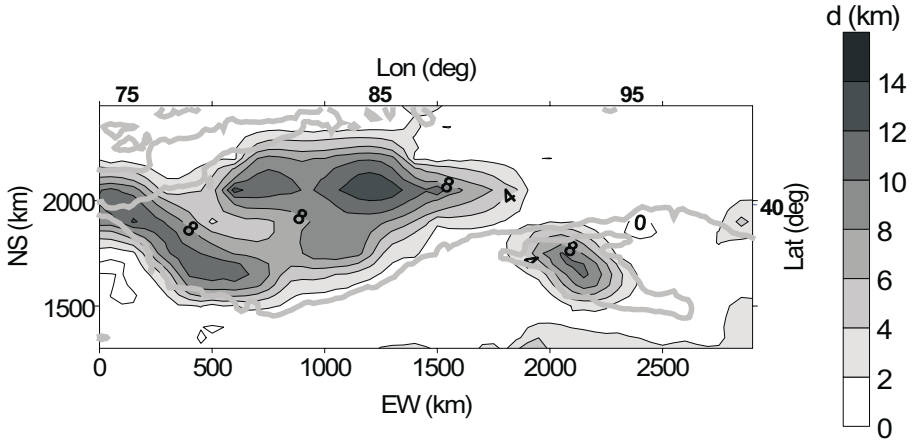

Fig. 3. Model of sediment basin thickness for the Tarim and Qaidam basins. The 3000 m topographic isoline has been added (gray line).

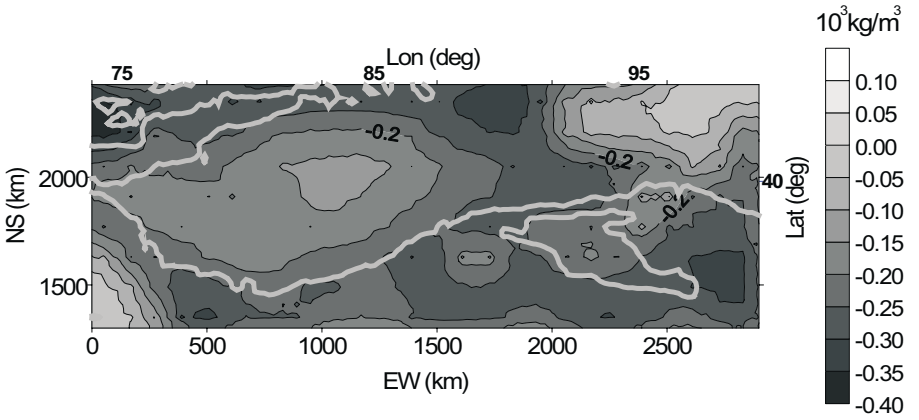

Fig. 4. Model of mean density of the sediment basin column for the Tarim and Qaidam basins. The 3000 m topographic isoline has been added (gray line).

thickness is mapped. The maximum thickness of the Tarim basin is 15 km. In the northwestern part a shallowing of the basin is present, with depths to about 4 km. On the flanks of this area the basin steeply falls towards the Tien Shan in the North and towards the Kun Lun range towards the South. The Qaidam basin is smaller in extent and has a depth of 10 km. Also a density model is available and shown in Fig. 4, and refers to the mean density in a column extending from the base to the surface. The density modeling was obtained from the integration of geological and geophysical investigations and borehole measurements (IGG-CAS database and [34]). The forward modeling was made by dividing the basin in thin horizontal slices, the gravity effect of which was evaluated by upward continuation. This procedure is considerably faster than by discretization with prisms. The gravity effect of the two basins is given in Fig. 5. The gravity values mainly reflect the varying depths of the two basins. For the Tarim the greatest values are found in the southern and northeastern part, where values reach -100 mgal (1 mgal $= 10^{-5}$ m/s^2), for the Qaidam basin the correction is also considerable and is up to -96 mgal.

3.2. The undulations of the CMI

The gravity effect of lithospheric thickening is modeled separately, adopting the lithospheric thickness model of Zhou et al. [35], and a density

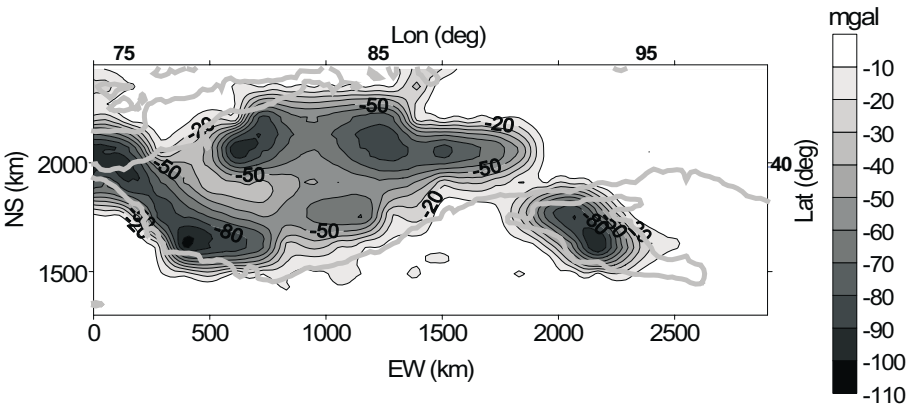

Fig. 5. Gravity effect of Tarim and Qaidam basins. The 3000 m topographic isoline has been added (gray line).

contrast of lithosphere to asthenosphere of 0.04×10^3 kg/m^3. Details on the lithospheric model and on the modeling can be found in Braitenberg et al. [7,8].

The gravity field of the basin model and of the lithospheric thickening is used to prepare the observed Bouguer field for the CMI gravity inversion, obtaining the values graphed in Fig. 6. The corrected Bouguer values over the central part of Tibet are between −500 and −600 mgal, having lesser values in the Tarim (between −100 and −200 mgal) and towards the Qaidam basin (between −400 and −500 mgal).

The corrected Bouguer field, which is stripped from the effects of the Tarim and Qaidam basins and of lithospheric thickening, is used in the gravity inversion of the CMI undulations, repeating the procedure described in Braitenberg et al. [7,8]. The CMI is modeled as a continuous plane of constant density contrast. From a technical point of view, laterally varying densities could be introduced into the model, but the complete lack of constraining information does not allow such a procedure. The inversion procedure depends on the CMI reference depth, which is the depth of the CMI for null Bouguer anomalies and on the vertical density contrast across the interface. In Braitenberg et al. [7,8] different couples of the CMI reference depth and the density contrast were tested, by controlling the solution with the constraining data. The best agreement was found for the reference depth d equal to 35 km and the density contrast across the interface equal to -0.4×10^3 kg/m^3.

The solution for the CMI variations according to the gravity inversion is shown in Fig. 7. Over the greater part of the plateau, the CMI is at a depth between 67 and 74 km. The Tarim basin has a shallower CMI with values between 40 and 50 km, for the Qaidam basin the CMI is at a depth of approximately 60 km.

4. Flexural modeling

The isostatic flexure modeling is fulfilled by applying the sum of the topographic and crustal load to the thin plate model. The flexure is computed by applying the convolution product of the load with the flexure response function characterized by a certain value of the flexure parameter T_e and the model parameters given in Table 1. The

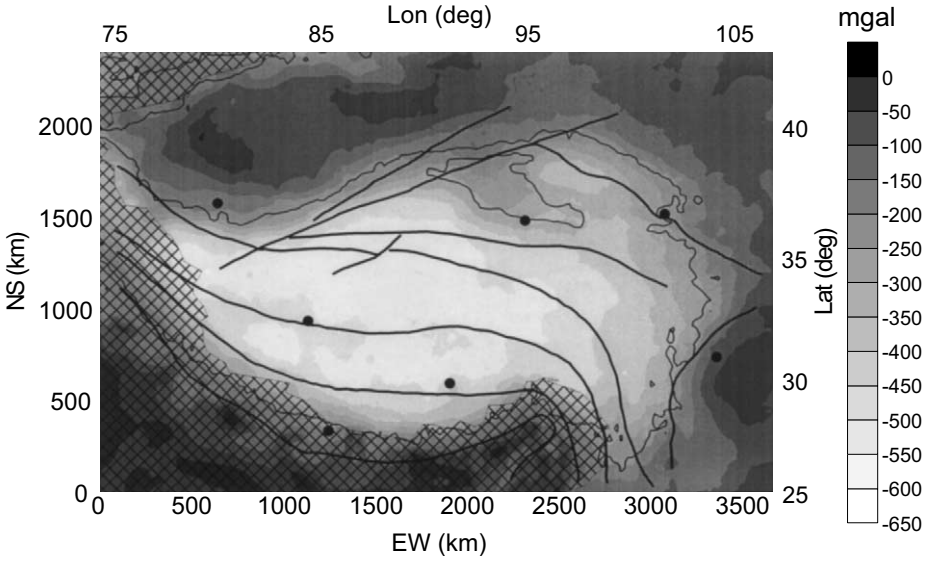

Fig. 6. Bouguer gravity field over Tibet–Quinghai plateau, corrected for lithosphere and sediment basins. This field is used for the gravity inversion. The hatching marks the area where no point gravity data were available. Towns, main tectonic lines and 3000 m topographic isoline have been added.

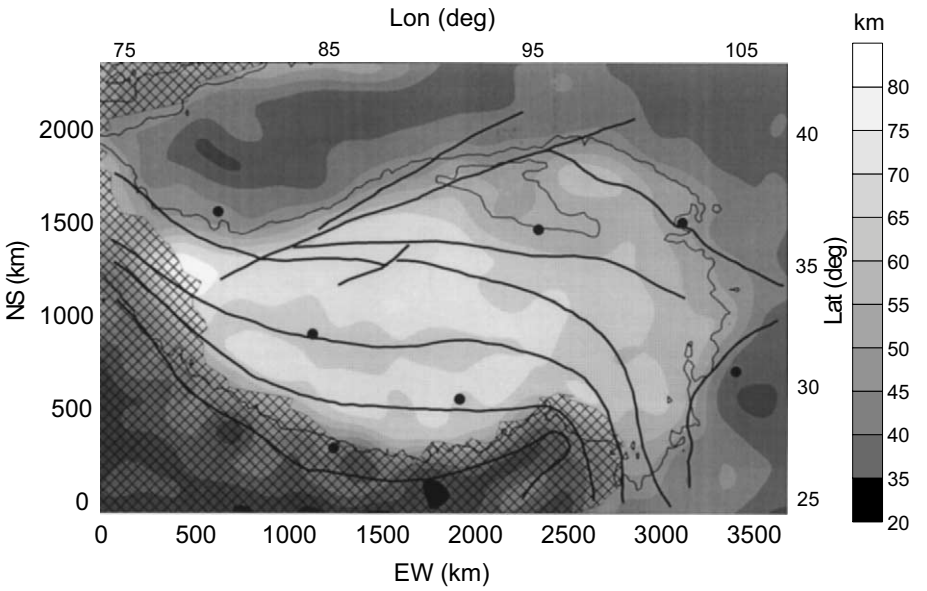

Fig. 7. CMI undulations obtained from the constrained gravity inversion and forward modeling. Hatched area, towns, tectonic lines and 3000 m topographic isoline as in Fig. 6.

flexed surface is compared to the CMI obtained in the previous paragraph by the constrained gravity inversion. The flexure parameter T_e is tuned so as to obtain the minimum of the rms difference between the flexure and the gravity CMI. The analysis is carried out on square windows of side length L that are shifted by the quantity W in order to cover the entire investigated area. The side length L determines the spatial resolution with which the T_e is modeled. Tests made on a synthetic numerical model representing the Eastern Alps, found that a small value of L leads to unstable results, and big values of L mask existing spatial variations of T_e, so a trade-off between the two values should be found. In the case of the synthetic model, a reasonable value of L was found to be 120 km. For the Tibet area we have tested overlapping square windows of 120–250 km side length shifted by one third of L. We find that a value of 250 km is adequate for the conditions of the Tibet area. The larger size with respect to the synthetic tests is explainable by the fact that the grid sampling in Tibet is 20 km, whereas the synthetic model was available at 5 km, in which latter case the number of values that enter the rms evaluation is greater.

Table 1
Parameters used in the flexural modeling

Mantle density	ρ_m	3.1×10^3 kg/m^3
Crustal density	ρ_c	2.7×10^3 kg/m^3
Young modulus	E	10^{11} Pa
Poisson ratio	σ	0.25
Grid spacing	dx,dy	20 km
Grid size CMI	Lx,Ly	2280 km by 3640 km
Grid size Topo	Lx,Ly	3600 km by 5600 km

The load is given by the sum of the topographic load and the inner-crustal loads. The topographic load is equal to the product of the topographic height and the density of 2.7×10^3 kg/m^3, the same as used for the topographic reduction.

The calculation of the inner-crustal loads is done in vertical columns, and in the general case of a layered crust is expressed by:

$$L_{\text{buried}} = \sum_{i=1}^{N} h_i \rho_i - \sum_{i=1}^{N} h_i \rho_c \quad (4)$$

with L_{buried} inner-crustal loads, h_i thickness of the ith layer, ρ_i density of the ith layer and ρ_c the

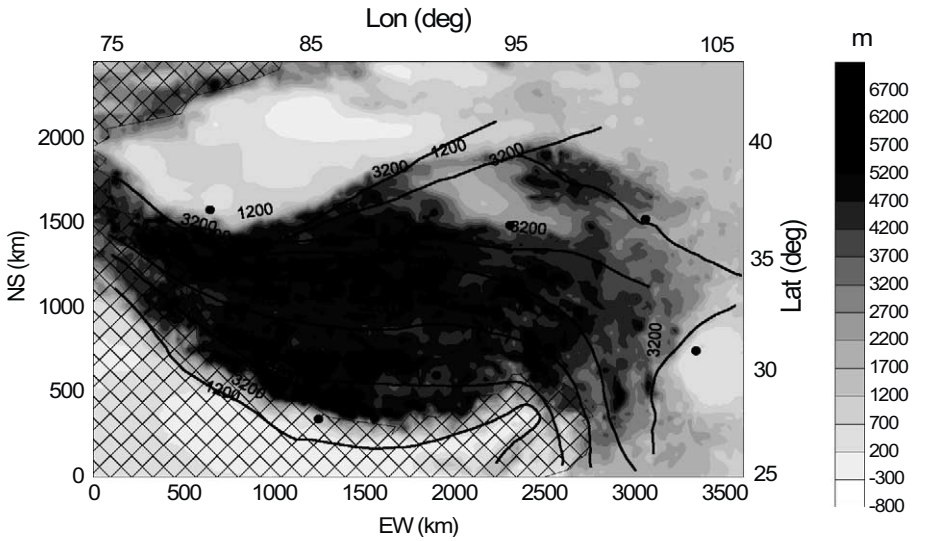

Fig. 8. Total load given by the sum of topographic and inner-crustal loads over the Tibet–Quinghai plateau expressed in terms of pseudotopography. Hatched area, towns and tectonic lines as in Fig. 6.

density of the reference crust. In our model the crustal reference density is equal to 2.7×10^3 kg/m^3, and the buried load is confined to the sedimentary basin. In Fig. 8 a plot of the total equivalent topography is made, which is the sum of the topographic and subsurface loads divided by the crustal density. The inner-crustal loads refer to the Tarim and Qaidam sedimentary basins. The resulting spatial variations of T_e are plotted in Fig. 9a, the resulting flexure CMI undulations in Fig. 9b, and the residual CMI undulations (flexure CMI minus gravity CMI) in Fig. 9c. The greater part of the Tibet–Quinghai plateau is found to have a T_e between 11 and 20 km. Lower values of near to 8 km are found for the Qiang Tang terrain and in the area limited by the Kunlun fault to the South, the Altyn Tagh line to the North, and the Qaidam basin to the East. The part of the Qiang Tang terrain that bends southwards in the eastern part of the plateau is found to have higher values of T_e, between 20 and 40 km. The Qaidam basin has high T_e between 50 and 70 km, the greater part of the Tarim basin even higher values up to 110 km. The Tarim basin is found to have the lowest values of T_e in its southwestern part (between 30 and 20 km), in correspondence to the area where the base of the basin shallows to a depth of near to 4 km (see Fig. 3). The flexure CMI resembles the gravity CMI very closely, as can be verified by comparison of Figs. 7 and 9b. The absolute difference between the two depths is mostly limited to values between ±3 km, as is shown in Fig. 9c.

5. Discussion and conclusion

The Chinese–Italian exchange program FLEXOLIT started in 1997 and has produced a unique opportunity to study the gravity field over the entire Tibet–Quinghai plateau. In a previous study [7,8], a first model of the CMI was formulated over the Tibet–Quinghai plateau and the Tarim basin, using all available results from seismic investigations and performing a constrained gravity inversion. In the present paper this CMI model was further improved in correspondence of the Tarim and Qaidam basins, as the two basins were modeled by forward gravity modeling, adopting existing data on the depth and the mean density of the basins. The correction amounts to approximately 5 km and produces a shallower CMI beneath the basins. The CMI reflects a model in which the density contrast across the interface is constant, an assumption that must be withheld, until sound geophysical arguments

are found that rebut this hypothesis and allow quantifying the variations in density. The CMI is found to be at a depth between 70 and 75 km over most of the plateau. The Yarlung Zangbo suture has a deep CMI (75 km), with a shallowing to values between 65 and 70 km along the Bangong Nujiang suture. The shallowing of the CMI is paralleled in the topography, which is characterized by a depression of near to 500 m along the suture. This upwarping of the CMI along the suture was found previously and related to the conversion process of the Indian and Eurasian plates by Jin et al. [18] and in a recent revision of all available seismologic recordings along the profile AA′ (Fig. 1) [36]. In the northeastern part of Tibet, comprising the Songpan terrain and the area limited by the Altyn Tagh line and the Kun Lun fault, the CMI shallows, with smallest depth val-

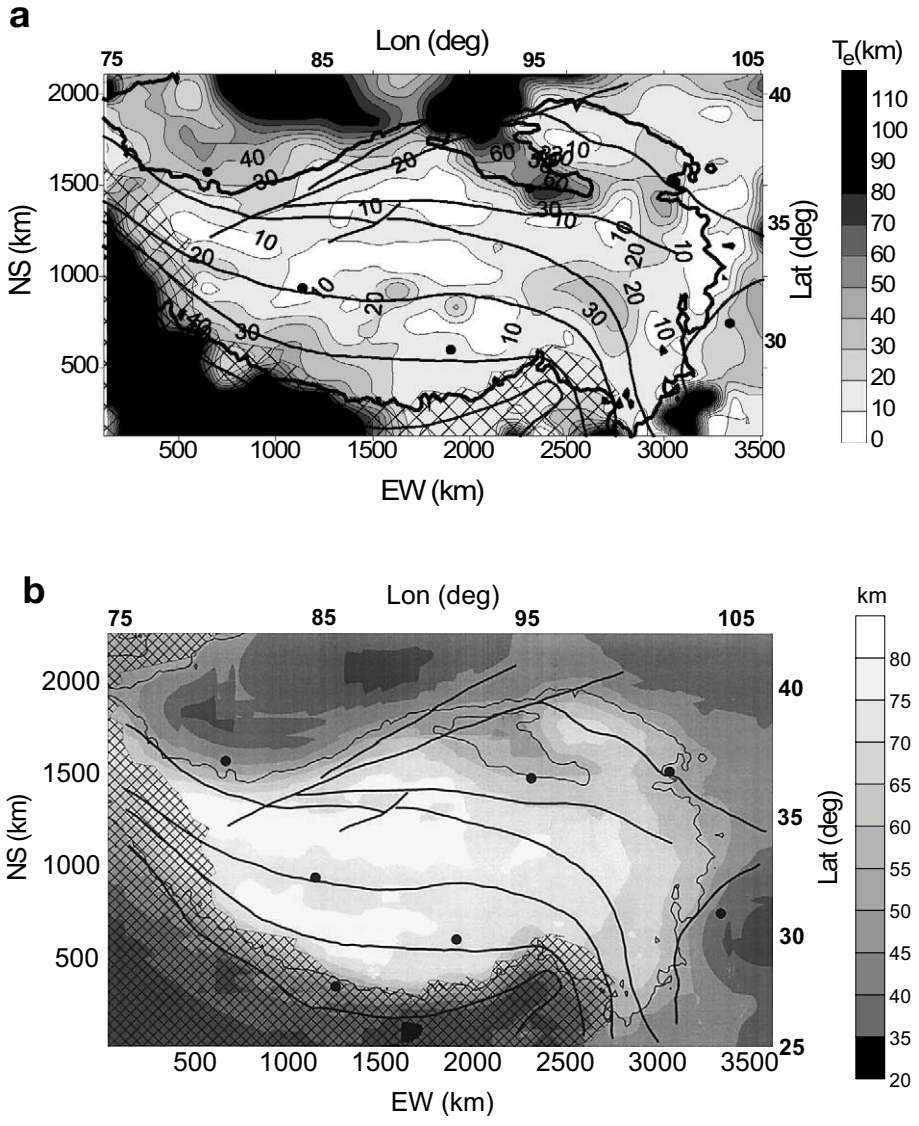

Fig. 9. Results from the lithospheric flexure model. (a) Lateral elastic thickness variations. (b) Depths of the CMI according to the flexural loading. (c) Difference between the flexure and gravity CMI undulations (positive: flexure CMI deeper than gravity CMI). Hatched area, main tectonic lines, towns and 3000 m topographic isoline as in Fig. 6.

ues below the Qaidam basin (near to 60 km). The Tarim basin has a shallow CMI, with values between 40 and 50 km. The structure we find for the CMI correlates with a number of other geophysical observations that have been made along profiles or in isolated investigation points. Kao-Honn et al. [37] characterize the Tarim basin with a crust with a depth of 42 km, dipping southwards towards a depth of 50 km. Regarding the N-Tibet and Qaidam basins, teleseismic recordings were interpreted with seismic tomography by Wittlinger et al. [38]. The study gives a mean crustal thickness of 54 km for the Qaidam basin.

The CMI obtained from the gravity inversion is used to estimate variations in the flexural properties of the Tibet plateau. We apply the thin plate flexure model loaded by the topographic and inner-crustal loads. The spatial resolution at which the flexural rigidity is obtained is very high (250 km) due to the convolution approach, overcoming the need to calculate the admittance and coherence functions of the gravity field and the load or alternatively of the CMI and the load. The convolution method [24] was tested on a synthetic model situation and was shown to be a valid means to recover spatial variations of flexural properties with a higher resolution compared to the admittance approach. We express the flexural properties of the plateau in terms of lateral variations of T_e.

When applied to the Tibet–Quinghai plateau and the Tarim basin, the resulting map of T_e reveals dramatic differences in the different terrains. The Tibet–Quinghai plateau has a T_e of 10–30 km, with a lowering to 8 km found in the Qiang Tang terrain and north of the Kun Lun fault. Very much higher values are found for the Tarim (up to 110 km) and the Qaidam basins (up to 70 km). Burov and Diament [20] undertake a modeling of T_e in different situations taking the yield stress envelope of the lithosphere into account. One major controlling factor is the mechanical decoupling of crust and mantle, which leads to a drastic reduction of the value of T_e. In the case of a layered model of the lithosphere, the T_e is given by an approximate relation that depends on the depth of the CMI (h), the depth below which the crustal part of the lithosphere is ductile (h_1) and the depth below which the mantle part of the lithosphere is ductile (h_2). The relation is [20]:

$$T_e = \sqrt[3]{h_1^3 + (h_2 - h)^3} \sim \max(h_1,\ h - h_2) \qquad (5)$$

The thickness h_1 is greatly controlled by the geo-

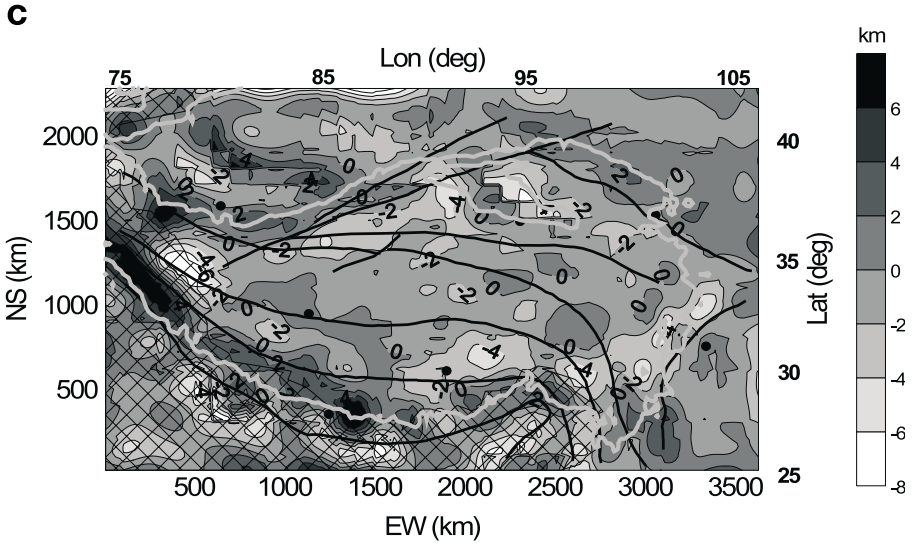

Fig. 9 (*Continued*).

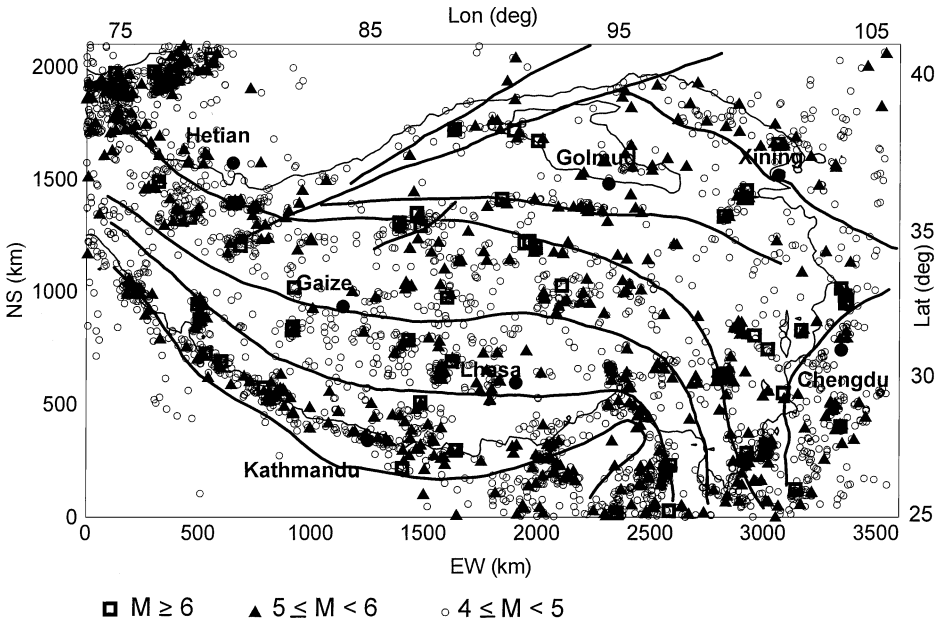

Fig. 10. Seismicity for the years 1980(Jan)–1992(March) over the Tibet–Quinghai plateau. Circles for events with magnitude $4 \leq M < 5$, triangles for $5 \leq M < 6$, and squares for $M \geq 6$ [42]. Main tectonic lines, rivers and towns have been added.

thermal gradient, with a shallowing for steeper gradients.

A recent compilation of heat flow data in China mainland, including Tibet, has been made by Wang [39]. The Tarim basin (45 mW/m^2) and the Qaidam basin (54 mW/m^2) have low heat flow, with respect to the Southern Tibet flow (82 mW/m^2). The Qiang Tang fold belt is also found to have a low heat flow value of 45 mW/m^2. Our findings regarding the T_e variations correlate well with the heat flow values, in that the high heat flow of most of Tibet correlates with the low T_e values, and the high T_e values of the Tarim and Qaidam basins correlate with the lower heat flow values. An exception to this correlation is found in the Qiang Tang belt, where we obtain low T_e values, but heat flow is also low. Presently the characterization of the Qiang Tang heat flow relies on one single heat flow measurement, and it cannot be ruled out that the low value pertains to a local anomaly. The low T_e values found for the Tibet plateau comply with the findings from MT (Magnetotelluric) surveys that interpreted the unusually high midcrustal electrical conductivity extending across the Lhasa block and the Qiang terrain with the presence of partial melt along grain boundaries. The top of the midcrustal conductive layer along the SW–NE trending profile passing through Lhasa and Golmud was found to be between 15 and 25 km depth [40]. We find higher T_e values in the eastern part of the Qiangtang terrain, across the Jinsha suture. Our findings indicate that a structural change occurs in this area, along with a southward bending of the main structural features. Apart from the low heat flow values, the high T_e found for the Tarim basin correlates well with other properties, such as the seismicity, geological considerations and the recent deformation revealed by GPS. The Tarim basin is known to be near to aseismic and to deform relatively little. This has been proposed before to be tied to the fact that its strength is higher than the one of its surrounding areas [41]. Theoretical modeling using a viscous layer acted on by a rigid block indenter showed that an increase in strength would predict a relatively low lying area, a normal thickness crust surrounded by higher topography and thicker crust, with rel-

atively small strain rates and total strain within the basin [42]. Interpretation of recent GPS observations has shown that the Tarim basin has very little inner deformation, and rotates like a rigid block [43]. A map of the seismicity for the period January 1980 to March 2002 gives a confirmation of the fact that the Tarim basin hardly deforms (Fig. 10), where all events with $M \geq 4$ are displayed. Circles refer to events with magnitude $4 \leq M < 5$, triangles to $5 \leq M < 6$, and squares to $M \geq 6$, according to the catalog published by NEIC [44]. It can be seen that the Tarim basin is near to being aseismic, although seismicity is strong along its margins. Also the Qaidam basin has low values of seismicity, compared with its surrounding areas. The high T_e values of the Tarim basin conform to other cratonic areas [20].

Our study has shown that the crustal model obtained from constrained gravity inversion and forward modeling leads to a consistent model in terms of lithospheric flexure. The depth to the CMI obtained from the gravity study is in good agreement (mostly within 3 km) with the undulations of the CMI expected for the flexural model, which has spatially varying elastic thickness T_e. The elastic thickness variations we find definitely separate the Tarim and Qaidam basins from the Tibet–Quinghai plateau, as the two basin structures appear to be much more rigid with respect to the Tibetan crust. Although the Tibetan crust is much thicker than the basins, it has low elastic thickness values, which is in accordance with the observations of heat flow, seismic velocities and electrical resistivity which have been interpreted due to the presence of a partially molten mid-crust.

Acknowledgements

The research has been made possible by a CAS-CNR exchange program between the Department of Earth Sciences of the Trieste University and the Institute of Geodesy and Geophysics of the Chinese Academy of Sciences (KZCX2-106/109). It has been mainly carried out during stays of C.B. in Wuhan and J.F. and Y.W. in Trieste. Prof. M. Zadro is thanked for discussions.*[AC]*

References

[1] G. Wu, X. Xiao, T. Li, Yadong to Golmud transect, Qinghai-Tibet plateau, China, Global Geoscience Transect 3, AGU, Publication No. 189 of the International Lithosphere Program, 1991, pp. 1–32 and supplementary foldout.

[2] A. Hirn, A. Nercessian, M. Sapin, G. Jobert, X.Z. Xin, G.E. Yuan, L.D. Yuan, J. Teng, Lhasa block and bordering sutures – a continuation of a 500-km Moho traverse through Tibet, Nature 307 (1984) 25–27.

[3] K.D. Nelson, W. Zhao, L.D. Brown, J. Kuo, J. Che, X. Liu, S.L. Klemperer, Y. Makovsky, R. Meissner, J. Mechie, R. Kind, F. Wenzel, J. Ni, J. Nabelek, Partially molten middle crust beneath southern Tibet Synthesis of Project INDEPTH results, Science 274 (1996) 1684–1688.

[4] R. Kind, J. Ni, W. Zhao, J. Wu, X. Yuan, L. Zhao, E. Sandvol, C. Reeses, J. Nabelek, T. Hearn, Evidence from earthquake data for a partially molten crustal layer in Southern Tibet, Science 274 (1996) 1692–1694.

[5] C.J. Allègre, V. Courtillot, P. Tapponier, A. Hirn, M. Mattauer, C. Coulon, J.J. Jaeger, J. Achache, U. Schärer, J. Marcoux, J.P. Burg, J. Girardeau, R. Armijo, C. Gariépy, C. Göpel, T. Li, X. Xiao, C. Chang, G. Li, Structure and evolution of the Himalaya-Tibet orogenic belt, Nature 307 (1984) 17–22.

[6] S. Li, W.D. Mooney, Crustal structure of China from deep seismic sounding profiles, Tectonophysics 288 (1998) 105–113.

[7] C. Braitenberg, M. Zadro, J. Fang, Y. Wang, H.T. Hsu, Gravity inversion in Quinghai-Tibet plateau, Phys. Chem. Earth 25 (2000) 381–386.

[8] C. Braitenberg, M. Zadro, J. Fang, Y. Wang, H.T. Hsu, The gravity and isostatic Moho undulations in Qinghai-Tibet plateau, J. Geodyn. 30 (2000) 489–505.

[9] A.B. Watts, Isostasy and Flexure of the Lithosphere, Cambridge University Press, Cambridge, 2001, 458 pp.

[10] H. Lyon-Caen, P. Molnar, Gravity anomalies and the structure of western Tibet and the southern Tarim basin, Geophys. Res. Lett. 11 (1984) 1251–1254.

[11] A. Caporali, Gravity anomalies and the flexure of the lithosphere in the Karakoram, Pakistan, J. Geophys. Res. 100 (1995) 15075–15085.

[12] A. Caporali, Buckling of the lithosphere in western Himalaya; constraints from gravity and topography data, J. Geophys. Res. 105 (2000) 3103–3113.

[13] A. Caporali, Gravimetric constraints on the rheology of the Indian and Tarim plates in the Karakoram continent-continent collision zone, J. Asian Earth Sci. 16 (1998) 313–321.

[14] H. Lyon-Caen, P. Molnar, Constraints on the structure of the Himalaya from an analysis of gravity anomalies and a flexural model of the lithosphere, J. Geophys. Res. 88 (1983) 8171–8191.

[15] G.D. Karner, A.B. Watts, Gravity anomalies and flexure of the lithosphere at mountain ranges, J. Geophys. Res. 88 (1983) 10449–10477.

[16] L.H. Royden, The tectonic expression slab pull at continental convergent boundaries, Tectonics 12 (1993) 303–325.
[17] Y. Jin, M.K. McNutt, Y. Zhu, Evidence from gravity and topography data for folding of Tibet, Nature 371 (1994) 669–674.
[18] Y. Jin, M.K. McNutt, Y. Zhu, Mapping the descent of Indian and Eurasian plates beneath the Tibetan Plateau from gravity anomalies, J. Geophys. Res. 101 (1996) 11275–11290.
[19] E.B. Burov, M. Diament, Flexure of the continental lithosphere with multilayered rheology, Geophys. J. Int. 109 (1992) 449–468.
[20] B. Burov, M. Diament, The effective elastic thickness (Te) of continental lithosphere: what does it really mean?, J. Geophys. Res. 100 (1995) 3905–3927.
[21] A.B. Watts, J.R. Cochran, G. Selzer, Gravity anomalies and flexure of the lithosphere: a three-dimensional study of the Great Meteor seamount, Northeast Atlantic, J. Geophys. Res. 80 (1975) 1391–1398.
[22] A. Cazenave, B. Lago, K. Dominh, K. Lambeck, On the response of the ocean lithosphere to sea-mount loads from Geos 3 satellite radar altimeter observations, Geophys. J. R. Astron. Soc. 63 (1980) 233–252.
[23] D.L. Turcotte, L. Schubert, Geodynamics, Applications of Continuum Physics to Geological Problems, John Wiley and Sons, New York, 1982, 450 pp.
[24] C. Braitenberg, J. Ebbing, H.-J. Götze, Inverse modelling of elastic thickness by convolution method – the eastern Alps as a case example, Earth Planet, Sci. Lett. 202 (2002) 387–404.
[25] C. Braitenberg, M. Zadro, Iterative 3D gravity inversion with integration of seismologic data, Boll. Geofis. Teor. Appl. 40 (1999) 469–476.
[26] C. Braitenberg, F. Pettenati, M. Zadro, Spectral and classical methods in the evaluation of Moho undulations from gravity data: the NE Italian Alps and isostasy, J. Geodyn. 23 (1997) 5–22.
[27] M. Zadro, C. Braitenberg, Spectral methods in gravity inversion: the geopotential field and its derivatives, Ann. Geofis. XL (1997) 1433–1443.
[28] J. Ebbing, C. Braitenberg, H.-J. Götze, Forward and inverse modelling of gravity revealing insight into crustal structures of the Eastern Alps, Tectonophysics 337 (2001) 191–208.
[29] C. Braitenberg, R. Drigo, A crustal model from gravity inversion in Karakorum, in: Wu Bing (Ed.), Int. Symp. on Current Crustal Movement and Hazard Reduction in East Asia and South-East Asia, Wuhan, 4–7 November 1997, Symp. Proc., Seismological Press, Beijing, 1998, pp. 325–341.
[30] D.W. Oldenburg, The inversion and interpretation of gravity anomalies, Geophysics 39 (1974) 526–536.
[31] H. Granser, Nonlinear inversion of gravity data using the Schmidt-Lichtenstein approach, Geophysics 52 (1987) 88–93.
[32] A. Spector, F.S. Grant, Statistical models for interpreting aeromagnetic data, Geophysics 35 (1970) 293–302.
[33] Lithospheric Dynamic Atlas of China, China Cartographic Publishing House, Beijing, 1989.
[34] M.E. Artemjev, M.K. Kaban, V.A. Kucherinenko, G.V. Demanyanov, V.A. Taranov, Subcrustal density inhomogeneities of Northern Eurasia as derived from the gravity data and isostatic models of the lithosphere, Tectonophysics 240 (1994) 249–280.
[35] B. Zhou, J.S. Zhu, K.Y. Chun, Three dimensional shear wave velocity structure beneath Qinghai-Tibet and its adjacent area, Acta Geophys. Sin. 34 (1991) 426–441.
[36] G. Kosarev, R. Kind, S.V. Sobolev, X. Yuan, W. Hanka, S. Oreshin, Seismic evidence for a detached Indian lithospheric mantle beneath Tibet, Science 283 (1999) 1306–1309.
[37] Kao-Honn, Gao-Rui, Rau-Ruey-Juin, Shi-Danian, Chen-Rong-Yuh, Guan-Ye, F. Wu, Seismic image of the Tarim Basin and its collision with Tibet, Geology 29 (2001) 575G–578G.
[38] G. Wittlinger, F. Masson, G. Poupinet, P. Tapponnier, J. Mei, G. Herquel, J. Guilbert, U. Achauer, X. Guanqi, S. Danian, Lithoscope Kunlun Team, seismic tomography of northern Tibet and Kunlun: evidence for crustal blocks and mantle velocity contrasts, Earth Planet. Sci. Lett. 139 (1996) 263–279.
[39] Y. Wang, Heat flow pattern and lateral variations of lithosphere strength in China mainland; constraints on active deformation, in: I. Kukkonen, V. Cermak, B. Kennett (Eds.), Thermal Studies of the Earth's Structure and Geodynamics, Phys. Earth Planet. Int. 126 (2001) 121–146.
[40] W. Wenbo, M. Unsworth, A. Jones, J. Booker, T. Handong, D. Nelson, C. Leshou, L. Shenghui, K. Solon, P. Bedrosian, J. Sheng, D. Ming, J. Ledo, D. Kay, B. Roberts, Detection of widespread fluids in the Tibetan crust by magnetotelluric studies, Science 292 (2001) 716–718.
[41] P. Molnar, P. Tapponnier, A possible dependence of tectonic strength on the age of the crust in Asia, Earth Planet. Sci. Lett. 52 (1981) 107–114.
[42] P. England, G. Houseman, Role of lithospheric strength heterogeneities in the tectonics of Tibet and neighbouring regions, Nature 315 (1985) 297–301.
[43] B. Reigber, G.W. Michel, R. Galas, D. Angermann, J. Klotz, J.Y. Chen, A. Papschev, R. Arslanov, V.E. Tzurkov, M.C. Ishanov, New space geodetic constraints on the distribution of deformation in Central Asia, Earth Planet. Sci. Lett. 191 (2001) 157–165.
[44] NEIC (2002), USGS National Earthquake Information Center, http://neic.usgs.gov/neis/epic/epic.html.